

# Anticorrosion study based on the film formed by a green nano-assembled aspartic amino acid-reinforced polysaccharide monolayer; Thermodynamic study

Mohammad Noor Mohammad Beigi<sup>1\*</sup>, Hasan Noor Mohammad Beigi<sup>2</sup>

Received: 2025-02-12

Revised: 2025-02-30

Accepted: 2025-02-30

DOI: [10.61186/CNJ.2.4.409](https://doi.org/10.61186/CNJ.2.4.409)

<sup>1</sup>R&D of water treatment, MHN Integrated Investment company. Muscat. Sultanate of Oman

<sup>2</sup>Boiler Manufacturing Group and R&D of Corrosion. Paya Bokhar Markazi, Machine Sazi Arak, Arak, Iran

## Abstract

This work is intended to introduce a novel combination of aspartic amino acid and polysaccharide, which both act as corrosion inhibitors. Here, a corrosion inhibitor composition prepared by a cationic cetyltrimethylammonium bromide surfactant (CTAB) based-colloid system and an anticorrosion film formed by a nano-assembled aspartic-reinforced polysaccharide monolayer on the aluminum substrate surface were investigated. The complex dynamics of ionic interactions in aspartic acid in modulating micellization of CTAB and their impact on surfactant behavior in CTAB/aspartic amino acid systems is a highlight and novelty of this work and is characterized by DLS analysis. This discussion is believed to provide a framework to facilitate a better understanding of particular aspects of the corrosion limitations. The obtained results of the anti-corrosion study reveal that the corrosion inhibitor prepared based on the CTAB colloid solution system has high performance compared to the bulk of aspartic acid and polysaccharide. The effect of temperature and inhibitor concentration were investigated and based on the surface coverage ( $\theta$ ), the equilibrium constant of adsorption ( $K$ ), the standard free energy ( $\Delta G^{\circ}_{ads}$ ), the standard enthalpy ( $\Delta H^{\circ}_{ads}$ ), and the entropy of adsorption ( $\Delta S^{\circ}_{ads}$ ) were calculated.

**Keywords:** Anticorrosion, Aspartic amino acid, Polysaccharide, Methyl cellulose

## 1. Introduction

Corrosion engineering is an engineering specialty that applies scientific, technical, and engineering skills, and knowledge of natural laws and physical resources to design and implement materials, structures, devices, systems, and procedures to manage corrosion [1]. A corrosion inhibitor or anti-corrosive is a chemical compound added to a liquid or gas to decrease the corrosion rate of a metal that comes into contact with the fluid [2]. The effectiveness of a corrosion inhibitor depends on fluid composition and dynamics [1]. Corrosion inhibitors, when added in small quantities, reduce or completely prevent the corrosion process. They may be anodic, cathodic, or mixed type depending upon whether they control the anodic reaction, the cathodic reaction, or both anodic and cathodic reactions [3]. Natural corrosion inhibitors such as polysaccharides have gained significant attention in recent years due to their eco-friendly, cost-effective, and sustainable nature [4]. Among polysaccharides, active carboxyl groups include, for example, carboxymethyl cellulose and its sodium salt. The availability, environmental friendliness, thermal stability, and biodegradability of Na-carboxymethyl cellulose justify the development of new directions for its application [5,6]. Organic compounds containing heteroatoms (such as N, S, P, O) and multiple bonds in addition to some functional groups are considered to be the most effective corrosion inhibitors. It's also been reported that organic compounds containing -OH, -COOH, NH<sub>2</sub>, etc. are excellent corrosion inhibitors, especially in acidic media. Amino acids are environmentally friendly compounds [7]. They are completely soluble in aqueous media, can be produced with high purity at low cost, and are non-toxic. These properties would justify using them to inhibit corrosion. Aspartic acid can be used as an efficient corrosion inhibitor [8,9]. A colloid system is a mixture in which one substance consisting of microscopically dispersed insoluble particles is suspended throughout another substance [10-14]. Surfactants are widely used to form nano micelles as nanoreactor as soft templates to control the size and morphology of nanodroplets [15-18].

In this study, a green nano-assembled aspartic amino acid-reinforced polysaccharide is examined as a corrosion inhibitor for the aluminum surface in 1.0 HCl solution at 20, 30, 40, and 50 °C using the weight loss measurement. In this study, first, a nanocolloid of amino acid was prepared based on the cetyltrimethylammonium bromide surfactant (CTAB) surfactant nanomicelles. It was found that nano-assembled aspartic amino acid-reinforced polysaccharide possesses an excellent corrosion-inhibiting effect at the studied conditions compared to pure polysaccharide and aspartic acid as a control sample. The effect of temperature and inhibitor concentration were investigated and based on the surface coverage ( $\theta$ ), the equilibrium constant of adsorption ( $K$ ), the standard free energy ( $\Delta G^{\circ}_{\text{ads}}$ ), the standard enthalpy ( $\Delta H^{\circ}_{\text{ads}}$ ), and the entropy of adsorption ( $\Delta S^{\circ}_{\text{ads}}$ ) were calculated. The nano-assembled aspartic amino acid-reinforced polysaccharide is a promising active compound for the formulation of acidizing corrosion inhibitors.

## 2. Experimental

### 2.1. Materials

Methyl cellulose Polysaccharides (3500-5600 mPa·s) as a hydrophilic white powder was purchased from tcichemicals Co. CTAB surfactant, CaCl<sub>2</sub> and HCl were purchased from Merck CO. Aspartic amino acid was purchased from Danapharmedco. Glyceryl was purchased from Sadrashimi Co.

### 2.2. Preparation of a nano-assembled aspartic amino acid-reinforced polysaccharide corrosion inhibitor

First, a solution of the aspartic amino acid (900 ppm) was prepared by dissolving appropriate amount in 100 mL CTAB/water (0.02 M) and was stirred for 30 min for the formation a stable/clear solution [19,20]. For the preparation of a nano-assembled aspartic amino acid-reinforced polysaccharide corrosion inhibitor solution, an amount of polysaccharide hydrogel solution was formed by adding polysaccharide with a concentration about 75 Wt.% to the CTAB Nano micelles contained amino acid by adjusting the pH of the prepared solution about 10. Then a glyceryl linkage coupling agent (60 mg) was added and stirred for about 30 min, keeping the formed viscous reinforced polysaccharide solution in an inert environment until CaCl<sub>2</sub> (24 mg) was added. The prepared hydrogel solution is ready to use for anti-corrosion study.

### 2.3. Characterization

DLS analysis was used to determine the Z-average and particle size distribution histogram of nano-assembled aspartic amino acid-reinforced polysaccharide corrosion inhibitor using Better size Nanoptic 90. DLS is a fast and non-invasive tool used to measure particle size, size distribution and stability in solutions or suspensions.

### 2.4. Corrosion study based on the weight loss measurements

Before weight loss testing, the samples were mechanically abraded with Emery paper from 60 to 800 grits. The samples were thoroughly cleaned with distilled water, degreased with acetone, and dried at room temperature in a desiccator. The initial weight of the samples was noted and recorded. The pre-weighed samples in triplicate were submerged in a 1M HCl solution without and with various inhibitor concentrations (200 ppm, 400 ppm, 600 ppm, and 800 ppm) at several temperatures (20°C, 30 °C, 40 °C, and 50 °C) for 48 h. After the immersion process, the samples were removed, cooled to room temperature, dipped in a pickling solution (zinc dust + NaOH solution) for 1 min, washed with distilled water, then degreased with acetone, dried, and re-weighed. The corrosion rate ( $v$ ) and the inhibitor efficiency (%) of nano-assembled inhibitor and rate of corrosion ( $R_c$ ) were calculated using Equations (1) and (2), respectively [21].

$$\text{Inhibitor efficiency (\%)} = \frac{\text{weight loss (blank)} - \text{weight loss (inhibitor)}}{\text{weight loss (blank)}} \times 100 \quad (1)$$

$$R_c = \frac{W}{A \cdot t} \quad (2)$$

and wherein  $W$  is the weight loss of aluminum,  $A$  is the surface area of the aluminum substrate,  $t$  is the exposure time.

The surface coverage, was calculated using Eq. (3):

$$\theta = \text{Inhibitor efficiency} / 100 \quad (3)$$

To confirm the successful adsorption and coverage of the monolayer on the substrate surface, thermodynamic parameters and adsorption isotherms were also calculated. The equilibrium constant of adsorption ( $K$ ), the

standard free energy ( $\Delta G^{\circ}_{\text{ads}}$ ), the standard enthalpy ( $\Delta H^{\circ}_{\text{ads}}$ ), and the entropy of adsorption ( $\Delta S^{\circ}_{\text{ads}}$ ) were calculated as follows [21]:

The linear form of the Langmuir isotherm relates  $C/\theta$  to  $C$  in the following way:

$$\frac{C}{\theta} = \frac{1}{K} + C \quad (4)$$

wherein  $C$  is the concentration of reinforced inhibitor, and  $\theta$  is the fraction of surface covered and calculated from the inhibition efficiency. The equilibrium constant of adsorption ( $K$ ) determined from Equation (4) at different temperatures is used in the following Equations 5-7 [21] to determine  $\Delta G^{\circ}_{\text{ads}}$  (KJ/mol),  $\Delta H^{\circ}_{\text{ads}}$  (KJ/mol), and  $\Delta S^{\circ}_{\text{ads}}$  (J/mol K) respectively, as summarized in Table 2.

$$\Delta G^{\circ}_{\text{ads}} = -RT \ln(55.5K) \quad (5)$$

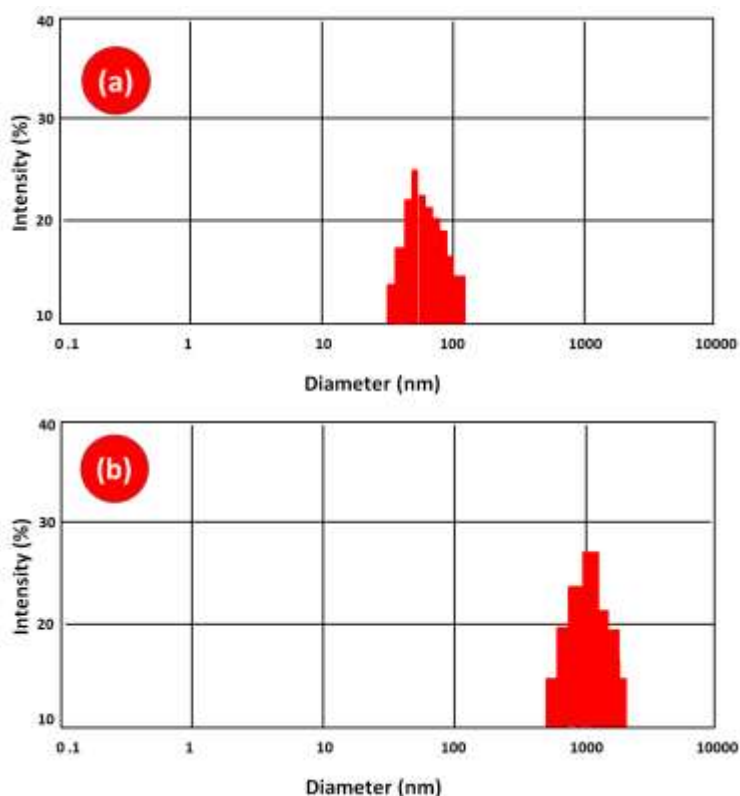
$$\ln K = \frac{-\Delta H^{\circ}_{\text{ads}}}{RT} + 1 \quad (6)$$

$$\ln K = \frac{-\Delta H^{\circ}_{\text{ads}}}{RT} + \left( \frac{\Delta S^{\circ}_{\text{ads}}}{R} - \ln 55.5 \right) \quad (7)$$

### 3. Results and discussion

#### 3.1. DLS

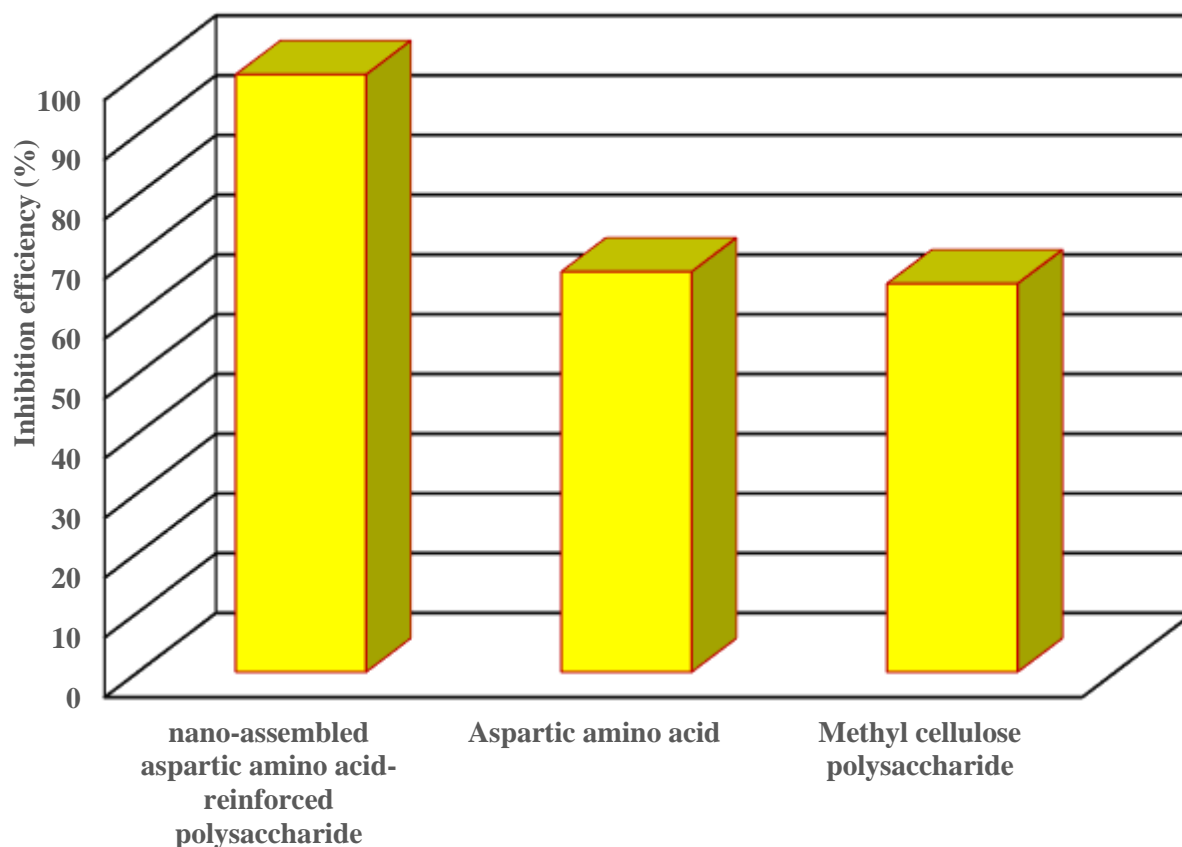
Fig. 1 (a and b) presents the DLS analysis of aspartic acid based CTAB nanocolloid and nano-assembled aspartic amino acid-reinforced polysaccharide inhibitor, respectively. DLS particle size analyzers are used to measure the size of very small particles (0.6 nm to 6  $\mu\text{m}$ ) in solution. The particle size range of DLS depends on the properties of the analyzed species, such as refractive index or density, as well as the surrounding formulation, mainly the viscosity. As can be seen, it is clear that the amino acid nanocolloid droplet size controlling is mainly dependent on surfactant, and when the CTAB surfactant concentration is 0.01 the nanodroplet particle size is 92 nm (Fig. 1-a). Based on intensity fluctuations of laser light scattered by the molecules/particles, moving in Brownian motion, the diffusion coefficient is determined and converted to particle size via the Stokes-Einstein equation. DLS can determine the hydrodynamic size of protein monomers, small aggregates in the nanometer range and partially also particles in the high nanometer/low micrometer range. The amino acid nanocolloid has excellent particle size distribution and monodispersity with the Z-average of 80 nm due to use of surfactant and micelles formation as nanocarrier [22-25]. Based on the Fig. 2-b, in the nano-assembled aspartic amino acid-reinforced polysaccharide inhibitor, the particle size is 1790 nm.



**Fig. 1.** DLS analysis of (a) aspartic acid based CTAB nanocolloid and (b) nano-assembled aspartic amino acid-reinforced polysaccharide inhibitor

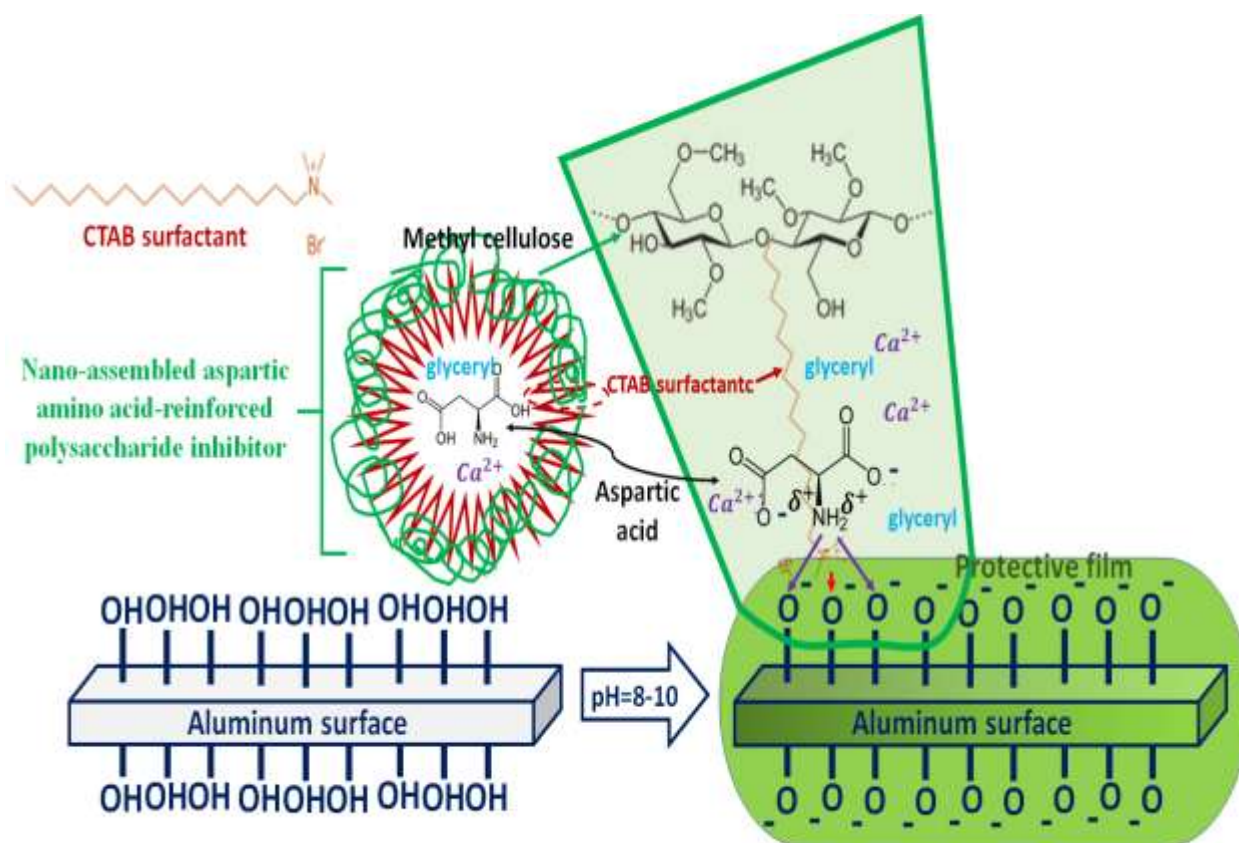
### 3.2. Anti-corrosion study

Fig. 2, presents the inhibition efficiency of nano-assembled aspartic amino acid-reinforced polysaccharide compared to the pure amino acid and methyl cellulose at room temperature while the concentration of inhibitors were adjusted at 800 ppm. As can be seen, the inhibition efficiency is more for nano-assembled aspartic amino acid-reinforced polysaccharide compared to the pure amino acid and methyl cellulose due to the synergistic effect of the nanomicelles contained- amino acid and methyl cellulose.



**Fig. 2.** The inhibition efficiency of nano-assembled aspartic amino acid-reinforced polysaccharide compared to the pure amino acid and methyl cellulose at room temperature with the inhibitor's concentration of 800 ppm after 48 h, (control study without each sample shows inhibition efficiency of 5.2%).

Based on the Fig. 3, it is clear that the inhibition efficiency of nano-assembled aspartic amino acid-reinforced polysaccharide monolayer, covering a surface of a substrate increases exponentially at a high nano-assembled aspartic amino acid-reinforced polysaccharide concentration and relatively low temperatures. Such inhibition increase denotes better-orientated monolayer constituents (i.e., zwitterion and reinforced nano-assembled aspartic amino acid-reinforced polysaccharide layers) over the substrate surface, and describes successive building up layer-by-layer of an anticorrosive shield over the substrate surface, hence configuring the surface to resist severe corrosive environments for prolonged time periods. It must be noted that the colloid system of amino acid with good monodispersity and shape/size form a uniform particle of nano-assembled aspartic amino acid-reinforced polysaccharide and this phenomenon caused to obtain a homogeneous layer on the surface of aluminum [26-29].



**Fig. 3.** Covering the surface of a substrate with nano-assembled aspartic amino acid-reinforced polysaccharide with better-orientated monolayer constituents (zwitterion and reinforced nano-assembled aspartic amino acid-reinforced polysaccharide layers) over the substrate surface, and describes successive building up layer-by-layer of an anticorrosive shield over the substrate surface

### 3.2.1. The effect of temperature and inhibitor concentration

It is also shown in Table 1 and Fig. 4, that inhibition efficiency and  $R_c$  decrease with rises in the system temperature and increase with rises the inhibitor concentration. The increase of inhibition and  $R_c$  with rises in inhibitor concentration is as expected considering the fact that the rate of a chemical reaction to produce film on the surface is accelerated at lower temperatures. Nevertheless, the decrease in inhibition and  $R_c$  is at a greater magnitude in the 1 M HCl solution without nano-assembled aspartic amino acid-reinforced polysaccharide as control sample than in the solution containing nano-assembled aspartic amino acid-reinforced polysaccharide, indicating the inhibiting effect of nano-assembled aspartic amino acid-reinforced polysaccharide with synergistic effect of polysaccharide and aspartic acid immobilized in CTAB nanomicelles [30-33]. The increases in  $\theta$  and inhibition efficiency with rises in inhibitor concentration are characteristics of an organic inhibitor that is adsorbed via a chemisorption mechanism with film forming [34,35]. Chemisorption involves an exchange of electrons between specific surface sites and inhibitor molecules or the transfer of electrons from the inhibitor molecule to the vacant orbital of the adsorbent, resulting in the formation of chemical bonds. Chemisorption bonds are stronger and more stable at high temperatures. The monolayer formation on the aluminum surface is meant to confirm and strengthen the firmness of the monolayer against a severe corrosive acidic environment for a prolonged time of exposure. Referring to Fig. 4, the shown inhibition efficiency values indicate that maximum inhibition ( $\approx 100\%$ ) is obtained for the 800 ppm reinforced polysaccharide concentrations. After the passage of about 48 hours, the monolayer is still preserving its skeleton, and no complete destruction or collapse of the bilayer occurred. This provides evidence on the strong intermolecular cohesive and adhesive forces within the bilayer itself and with the aluminum surface, which indicates the superior protection of the monolayer and the bilayer against a severe corrosive environment for a prolonged time period [21].

Table 1. The corrosion rate ( $v$ ) and the inhibitor efficiency (%) of nano-assembled inhibitor and rate of corrosion ( $R_c$ ) were calculated using Equations (1 and 2) at different temperature

Corrosion inhibitor concentration (ppm)	Temperature (K)	Normalized weight loss ( $\text{mg cm}^{-2}$ )	Rate of corrosion, ( $R_c$ ) $\times 10^6$ ( $\text{mg cm}^{-2} \text{s}^{-1}$ )
0	293	1.59	447
	303	2.78	802
	313	6.42	170
	323	6.76	181
200	293	0.145	46.3
	303	0.28	80.5
	313	0.99	289
	323	2.01	553
400	293	0.0543	14.6
	303	0.64	17.2
	313	1.02	27.8
	323	1.35	35.3
600	293	0.0302	5.77
	303	0.0410	10
	313	0.93	229
	323	0.789	241
800	293	0.00408	1.54
	303	0.0296	8.5
	313	0.842	237
	323	0.541	181

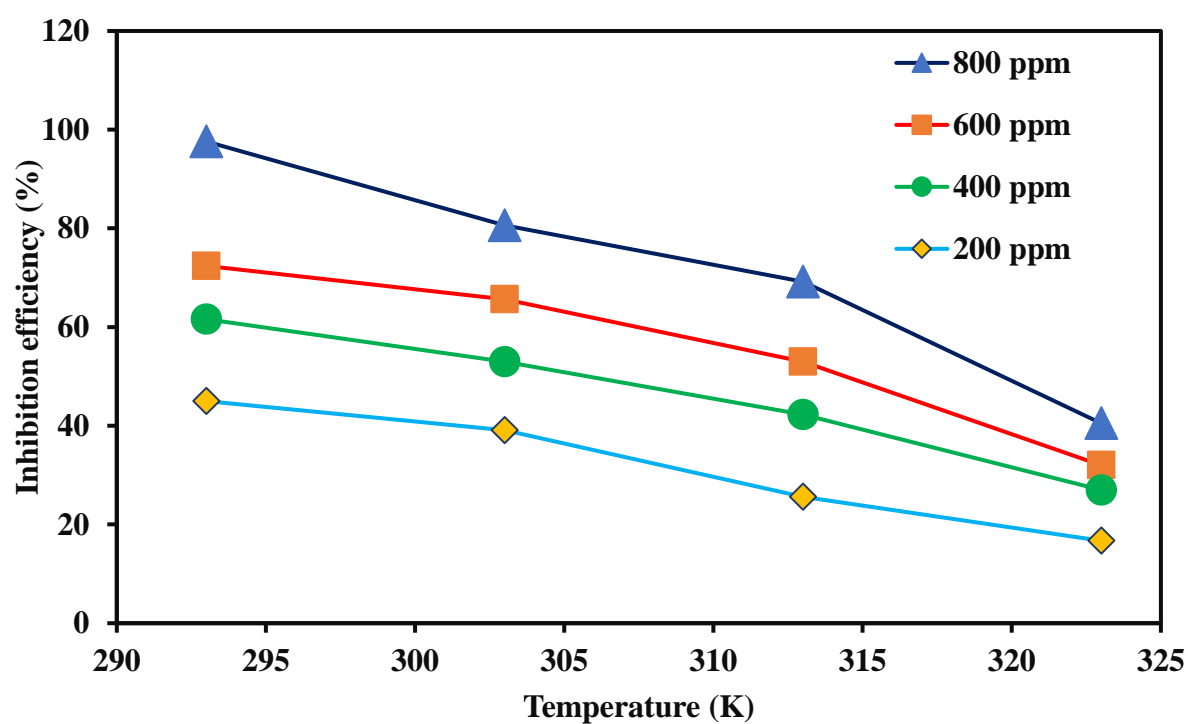


Fig. 4. Inhibition efficiency of nano-assembled aspartic amino acid-reinforced polysaccharide at different temperatures and inhibitor concentrations

### 3.2.2. Thermodynamic study

Thermodynamics is the study of the relations between heat, work, temperature, and energy. The laws of thermodynamics describe how the energy in a system changes and whether the system can perform useful work on its surroundings. Apparently, with nano-assembled aspartic amino acid-reinforced polysaccharide the absolute value of standard free energy of the adsorption of the anticorrosion film monolayer is in a range of 23-25 kJ/mol, which confirms that the monolayer adsorption on the metal surface is a physical adsorption process. In addition, at 50° C, the  $\Delta S^{\circ}_{\text{ads}}$  value decreased due to high surface energy that favors desorption of the monolayer (less entropic) and adsorption of water molecules (more entropic) on the metal surface as follows [21]:

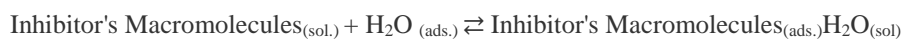


Table 2. The equilibrium constant of adsorption (K) determined from Equation (4) at different temperatures and calculated determine  $\Delta G^{\circ}_{\text{ads}}$ ,  $\Delta H^{\circ}_{\text{ads}}$ , and  $\Delta S^{\circ}_{\text{ads}}$  from Equation (5-7)

Temperature (K)	K (L g <sup>-1</sup> )	r <sup>2</sup>	$\Delta G^{\circ}$ (kJ mol <sup>-1</sup> )	$\Delta H^{\circ}$ (kJ mol <sup>-1</sup> )	$\Delta S^{\circ}$ (J mol <sup>-1</sup> K <sup>-1</sup> )
293	24.7	1.000	-24.1		57.2
303	20.5	0.978	-25.0	-8.65	56.4
313	18.2	0.989	-26.1		55.1
323	7.9	0.993	-23.9		49.3

### 3.2.3. Proposed mechanism

As can be seen from Fig. 3, which schematically illustrates how the aluminum oxide layer on the surface interacts with water to form a hydroxylated aluminum layer. The hydroxylated aluminum groups could be protonated or deprotonated depending on a selected pH value of the aqueous solution. Such protolytic equilibrium of hydroxylated aluminum can activate the aluminum surface with either positively or negatively charged ions. The zero -charge potential for the resultant aluminum surface lies between a pH of 6 to 9. Therefore, at pH=10, the aluminum surface is activated with negatively charged ions (Al—O<sup>-</sup>), while at pH=5, the aluminum surface is activated with positively charged ions [21]. a monolayer can be performed by dissolving inhibitor in distilled water and adjusting the pH of the solution to a pH of about 8.5, and soaking sheets of the substrate (aluminum with Al—O<sup>-</sup> surface) in solution. the amino acid in nanomicelles at a pH of about 8.5 is deprotonated from the carboxylic acid leading to a negative side of the carboxylate ion, and as a result a simultaneous attraction occurs of aluminum surface ions to the free partially positive hydrogen atoms of the amine groups in the aspartic acid, leading to the formation of a zwitterion layer over the substrate surface. Consequently, the negative side of the carboxylate ion of the aspartic acid will be oriented toward the solution. Surface of the polysaccharide microspheres are deprotonated at a pH of about 10, which can interact with a glyceryl linkage (C<sub>3</sub>H<sub>5</sub>ClO) to form a 3D network. The coupling of polysaccharide microspheres into the growing chain continues irregularly until reinforced methyl cellulose clusters are formed. The addition of calcium ions (Ca<sup>2+</sup>) cross-linked the zwitterion layer with the free methyl cellulose clusters and eventually formed a nano aspartic acid-reinforced methyl cellulose monolayer over the aluminum surface.

## 4. Conclusion

Here, a corrosion inhibitor composition based on the aspartic amino acid and methyl cellulose polysaccharide, which both act as corrosion inhibitor was introduced. A cationic cetyltrimethylammonium bromide surfactant (CTAB) based-colloid system was used to prepare nanomicelles of amino acid to control morphology and size of nanodroplet and characterized with DLS analysis. An anticorrosion film formed by a nano-assembled aspartic-reinforced polysaccharide monolayer on the aluminum substrate surface and inhibitor efficiency for all conditions based on the weight loss were measured. The complex dynamics of ionic interactions in aspartic acid in modulating micellization of CTAB and their impact on surfactant behavior in CTAB/aspartic amino acid systems is a highlight and novelty of this work. This discussion is believed to assist can be provided a framework to facilitate a better understanding of particular aspects of the corrosion limitations. The obtained results of anti-corrosion study reveal that the corrosion inhibitor prepared based on the CTAB colloid solution system has high

performance compared to the bulk of aspartic acid and polysaccharide. The effect of temperature and inhibitor concentration were investigated and based on the surface coverage ( $\theta$ ), the equilibrium constant of adsorption ( $K$ ), the standard free energy ( $\Delta G^\circ_{\text{ads}}$ ), the standard enthalpy ( $\Delta H^\circ_{\text{ads}}$ ), and the entropy of adsorption ( $\Delta S^\circ_{\text{ads}}$ ) were calculated. The obtained results indicate that coating type could prolong the life time of aluminum in aggressive  $\text{Cl}^-$  ion-containing solution, combining the protection effect of sacrificial inhibitor with barrier nanomicelles of amino acid and active polysaccharide protective effects.

### Conflicts of Interest

The authors declare that they have no known competing financial interests or personal relationships that could have appeared to influence the work reported in this paper.

### Author information

\*Corresponding Author: Mohammad Noor Mohammad Beigi

Email: [mbeygi.ir@gmail.com](mailto:mbeygi.ir@gmail.com)

### References

- [1] A. Thyagarajan, W. Hamer, J. Phophichitra, V. Valliappan, A. Ramesh, P. Shenai, N. Laycock, The virtual corrosion engineer. *Corros. Mater. Degrad.*, 2(4) (2021) 762-769. <https://doi.org/10.3390/cmd2040041>
- [2] Y. Sun, Surface engineering & coating technologies for corrosion and tribocorrosion resistance. *Materials*. 16(13) (2023) 4863. <https://doi.org/10.3390/ma16134863>
- [3] D. Jedrzejczyk, E. Szatkowska, The influence of heat treatment on corrosion resistance and microhardness of hot-dip zinc coating deposited on steel bolts. *Materials* 15 (2022) 5887.
- [4] A.V. Fakhreeva, V.V. Nosov, A.I. Voloshin, V.A. Dokichev, Polysaccharides as effective and environmentally friendly inhibitors of scale deposition from aqueous solutions in technological processes. *Polymers*. 15(6) (2023) 1478. <https://doi.org/10.3390/polym15061478>
- [5] H.M.S. Akhtar, S. Ahmed, E. Olewnik-Kruszkowska, M. Gierszewska, M.S. Brzezinska, K. Dembińska, A. Kalwasińska, Carboxymethyl cellulose based films enriched with polysaccharides from mulberry leaves (*Morus alba* L.) as new biodegradable packaging material. *Int J Biol Macromol*. 253(Pt 8) (2023) 127633. <https://doi.org/10.1016/j.ijbiomac.2023.127633>.
- [6] M.S. Lavlinskaya, A.V. Sorokin, Enhancement of water uptake in composite superabsorbents based on carboxymethyl cellulose through porogen incorporation and lyophilization. *Gels*, 10(12) (2024) 797. <https://doi.org/10.3390/gels10120797>
- [7] A. Kasprzhitskii, G. Lazorenko, T. Nazdracheva, V. Yavna V. Comparative computational study of l-amino acids as green corrosion inhibitors for mild steel. *Computation*, 9(1) (2021) 1. <https://doi.org/10.3390/computation9010001>
- [8] Y.I. Kuznetsov, Triazoles as a class of multifunctional corrosion inhibitors. Review. part II. 1,2,3-benzotriazole and its derivatives. *Iron and steels. Int. J. Corros. Scale Inhib.*, 9 (2020) 780–811. [[Google Scholar](#)] [[CrossRef](#)]
- [9] L. Hamadi, S. Mansouri, K. Oulmi, A. Kareche, The use of amino acids as corrosion inhibitors for metals: A review. *Egyptian Journal of Petroleum*, 27(4) (2018) 1157–1165. <https://doi.org/10.1016/j.ejpe.2018.04.004>
- [10] A. Salabat, B.S. Mirhoseini, F. Mirhoseini, Ionic liquid based surfactant-free microemulsion as a new protocol for preparation of visible light active poly(methyl methacrylate)/ $\text{TiO}_2$  nanocomposite. *Sci. Rep.*, 14 (2024) 15676. <https://doi.org/10.1038/s41598-024-66872-7>
- [11] F. Mirhoseini, A. Salabat, Antibacterial activity based poly(methyl methacrylate) supported  $\text{TiO}_2$  photocatalyst film nanocomposite, *Tech. J. Eng. Appl. Sci.* 5 (2015) 115-118.
- [12] Y. Tan, D.J. McClements, Plant-based colloidal delivery systems for bioactives. *Molecules*, 26(22) (2021) 6895. <https://doi.org/10.3390/molecules26226895>
- [13] F. Mirhoseini, Alireza Salabat, Ionic liquid based microemulsion method for fabrication of poly(methyl methacrylate)- $\text{TiO}_2$  nanocomposite as highly efficient visible light photocatalyst, *RSC Adv.* 5 (2015) 12536–12545. <https://doi.org/10.1039/c4ra14612c>
- [14] A. Salabat, F. Mirhoseini, Applications of a new type of poly(methyl methacrylate)/ $\text{TiO}_2$  nanocomposite as an antibacterial agent and a reducing photocatalyst. *Photochem. Photobiol. Sci.*, 14(9) (2015) 1637–1643. <https://doi.org/10.1039/c5pp00065c>

- [15] X. Qi, S. Simsek, B. Chen, J. Rao, Alginate-based double-network hydrogel improves the viability of encapsulated probiotics during simulated sequential gastrointestinal digestion: Effect of biopolymer type and concentrations. *Int. J. Biol. Macromol.* **2020**, 165 (2020) 1675–1685. [[Google Scholar](#)] [[CrossRef](#)] [[PubMed](#)]
- [16] F. Mirhoseini, A. Salabat, Removal of methyl tert -butyl ether as a water pollutant by photodegradation over a new type of poly(methyl methacrylate)/TiO<sub>2</sub> nanocomposite. *Polymer Composites*, 39(4) (2018) 1248–1254. <https://doi.org/10.1002/pc.24059>
- [17] A. Salabat, F. Mirhoseini, R. Valirasti, Engineering poly(methyl methacrylate)/Fe<sub>2</sub>O<sub>3</sub> hollow nanospheres composite prepared in microemulsion system as a recyclable adsorbent for removal of benzothiophene, *Ind. Eng. Chem. Research* 58 (2019) 17850-1785. <https://doi.org/10.1021/acs.iecr.9b04322>
- [18] F. Kamali, K. Faghihi, F. Mirhoseini, F. High antibacterial activity of new eco-friendly and biocompatible polyurethane nanocomposites based on Fe<sub>3</sub>O<sub>4</sub>/Ag and starch moieties. *Polym. Eng. Sci.*, 62(5) (2022) 1444-1462. <https://doi.org/10.1002/pen.25934>
- [19] A. Salabat, F. Mirhoseini, M. Arjomandzadegan, E. Jiryaei, A novel methodology for fabrication of Ag-polyppyrrrole core-shell nanosphere using microemulsion system and evaluation of its antibacterial application, *New J. Chem.* 41 (21) (2017) 12892–12900. <https://doi.org/10.1039/c7nj00678k>
- [20] A. Salabat, F. Mirhoseini, M. Mahdieh, H. Saydi, A novel nanotube-shaped polypyrrrole-Pd composite prepared using reverse microemulsion polymerization and its evaluation as an antibacterial agent, *New J. Chem.* 39 (5) (2015) 4109–4114. <https://doi.org/10.1039/c5nj00175g>
- [21] M.M. Fares, K.H. Masadeh, Glutamine-reinforced silica gel microassembly as protective coating for aluminium surface. *Mater. Chem Phys.*, 162 (2015) 124–130. <https://doi.org/10.1016/j.matchemphys.2015.05.042>
- [22] A. Salabat, F. Mirhoseini, Z. Masoumi, M. Mahdie, Preparation and characterization of polystyrene-silver nanocomposite using microemulsion method and its antibacterial activity, *JNS* 4 (2014) 377-382.
- [23] A. Salabat, F. Mirhoseini, Polymer-based nanocomposites fabricated by microemulsion method, *Polym. Compos.* 43 (2022) 1282–94.
- [24] F. Mirhoseini, A. Salabata, Investigation of operational parameters on the photocatalytic activity of a new type of poly(methyl methacrylate)/ionic liquid-TiO<sub>2</sub> nanocomposite, *Iranian J. Chem. Chem. Eng.*, 38 (2019) 101-114. <https://doi.org/10.30492/IJCCE.2019.37613>
- [25] B. Zeeb, L. Mi-Yeon, M. Gibis, J. Weiss, Growth phenomena in biopolymer complexes composed of heated WPI and pectin. *Food Hydrocoll.* 74 (2018) 53–61. <https://doi.org/10.1016/j.foodhyd.2017.07.026>
- [26] A. Salabat, F. Mirhoseini, K. Abdoli, A microemulsion route to fabrication of mono and bimetallic Cu/Zn/γ-Al<sub>2</sub>O<sub>3</sub> nanocatalysts for hydrogenation reaction. *Scientia Iranica*, 25(2018) 1364-1370. <https://doi.org/10.24200/sci.2018.5023.1048>
- [27] F. Mirhoseini, A. Salabata, Investigation of operational parameters on the photocatalytic activity of a new type of poly(methyl methacrylate)/ionic liquid-TiO<sub>2</sub> nanocomposite, *Iranian J. Chem. Chem. Eng.*, 38 (2019) 101-114. <https://doi.org/10.30492/IJCCE.2019.37613>
- [28] A. Salabat, F. Mirhoseini, F.H. Nouri, Microemulsion strategy for preparation of TiO<sub>2</sub>-Ag/poly(methyl methacrylate) nanocomposite and its photodegradation application. *J. Iranian Chem. Soc.* 20 (2022) 599–608. <https://doi.org/10.1007/s13738-022-02693-7>.
- [29] Noor Mohammad Beigi, M. Boosting the impact of cinnamaldehyde-contained polymer microemulsion on the corrosion of C1018 alloy in an acidic medium. *Colloid & Nanoscience Journal*, 2024; 2(1): 220-227. <https://doi.org/10.61186/CNJ.2.1.220>
- [30] Mirhoseini, B. S., Noor Mohammad Beigi, M. A novel nanocolloid system based on the poly(methyl methacrylate) nanoparticles as anticorrosive agent for boiler; a pilot -scale study. *Colloid Nanosci. J.*, 1(3) (2023) 139-146. <https://doi.org/10.61186/CNJ.1.3.139>
- [31] F. Mirhoseini, A. Salabat, Polymer nanocomposite based composition and method for controlling water hardness, United States patent 11136247.
- [32] F. Mirhoseini, A.Salabat, Photocatalytic filter, United States patent 10828629.
- [33] F. Mirhoseini, B.S. Mirhoseini, M. Noor Mohammad Beigi, M. Understanding the photodegradation of amoxicillin antibiotic using visible light sensitized poly(methyl methacrylate)/TiO<sub>2</sub> nanocomposite. *Nano Sci. Technol. J.* 1(1) (2023) 38-48. <https://doi.org/10.22034/nstj.2023.707804>

- [34] M. Hoseini, S. Hamidi, E. Salehi, A. Mohammadi, F. Mirhoseini, M. Ravaghi. Multi-variate multi-objective optimization of production conditions for electro-spun skin scaffold using RSM and investigation of gamma irradiation effects on the properties of the optimized sample. *Heliyon* 10 (12) (2024a) e3294.
- [35] A. Salabat, F. Mirhoseini, Photo-induced hydrophilicity study of poly(methyl methacrylate)/TiO<sub>2</sub> nanocomposite prepared in ionic liquid based microemulsion system. *Current Appl. Polym. Sci.*, 2(2), (2018) 112–120. <https://doi.org/10.2174/2452271602666180803141554>